View metadata, citation and similar papers at core.ac.uk

brought to you by CORE

provided by IntechOpen

We are IntechOpen, the world's leading publisher of Open Access books Built by scientists, for scientists

5,300
Open access books available

130,000
International authors and editors

155M
Downloads

Our authors are among the

154
Countries delivered to

TOP 1%
most cited scientists

12.2%
Contributors from top 500 universities

CLARIVATE ANALYTICS BOOK CITATION INDEX INDEXED

WEB OF SCIENCE™

Selection of our books indexed in the Book Citation Index in Web of Science™ Core Collection (BKCI)

Interested in publishing with us?
Contact book.department@intechopen.com

Numbers displayed above are based on latest data collected.
For more information visit www.intechopen.com

Chapter

Spectroscopy in Oilfield Corrosion Monitoring and Inhibition

Ekemini Ituen, Lin Yuanhua, Ambrish Singh and Onyewuchi Akaranta

Abstract

Interaction of surfaces of metals and alloys with electromagnetic radiation produces several interesting phenomena, including electronic transitions, molecular rotation and vibration within bonds, polarisation, or photochemical reactions. Spectroscopy is an essential tool that provides some structural information about these interactions. In corrosion, spectroscopic techniques are often employed for mechanistic determinations, especially in the presence of corrosion inhibitors. In this chapter, we have examined some spectroscopic methods that are useful for corrosion monitoring and corrosion inhibition. More emphasis is placed on sample preparation, output parameters, interpretation of results and possible deductions/predictions, which could be made from obtained results than on the underlying principles and mode of equipment operation. Attempts are also made to critically examine some literature, hence readers (early career researchers) and experts in the field will find this chapter very resourceful and a ready reference material.

Keywords: corrosion products, EDS, EIS, FTIR, UV-Vis, XRD

1. Introduction

Once existing wells begin to deplete, it becomes essential to use some principles of chemistry and materials science to maintain production through operations, such as well acidising, secondary and enhanced oil recovery. A common field technique for achieving this is to force a fluid (mixtures which could include acid, water and polymers) through the well bore at high pressure. This fluid dissolves formation rocks, enlarges existing flow channels and opens new ones by etching to enhance the flow of hydrocarbons. During this procedure, corrosion of steel structural materials often occurs. Such materials include line pipes, casings and tubings. After recovery, the spent acid could also cause corrosion of storage facilities. Problems associated with such corrosion could include rupturing of materials, spills, failure, loss of hydrocarbons and loss of materials' integrity and flow challenges. The cost of maintaining/cleaning spills is often high, hence most industries would find methods to prevent or retard corrosion. Also, the downtime due to the shutdown of plant for maintenance and damage to employees or company integrity is undesirable. The use of corrosion inhibitors (CIs) has been considered the simplest and cost-effective means of mitigating oilfield corrosion. Corrosion inhibitors (CIs) are chemical

substances which are added in small amounts to the corroding fluid in order to retard the speed of corrosive attack on the steel surface which it contacts [1].

Corrosion inhibitors offer surface protection by adsorption of their active functionalities on the substrate (steel) surface to 'blanket' it from the aggressive medium. The effectiveness or efficiency of the inhibitor varies as its chemical identity, composition, concentration and operational temperature and pressure varies [2, 3]. To estimate the efficiency or performance of CIs, techniques such as gravimetry, gasometry, adsorptiometry and electrochemistry have been used [1, 4]. The extent of protection, pitting and roughness (morphology) of the specimen surface is often checked using surface analytical techniques such as scanning electron microscopy (SEM) and atomic force microscopy (AFM), and it is usually different without and with the CI. The difference may be associated with monolayers or multilayers of adsorbed CIs on the surface. To understand the mechanism of interaction between the functionalities on the CI and the surface, various spectroscopic techniques have been used [5–7]. Such techniques include Fourier-transformed infrared spectroscopy (FTIR), atomic absorption spectroscopy (AAS), energy dispersive X-ray spectroscopy (EDS) and X-ray photoelectron spectroscopy (XPS).

Since most efficient CIs contain oxygen, nitrogen, sulphur, phosphorus, multiple bonds, aromatic and heterocyclic rings in their molecular structures [8, 9], the technique used is directed towards detecting the presence of these functionalities on the surface. The corroding environment also has to be taken into consideration. Typical corrosive environments include all forms of water, industrial, marine, neutral and urban atmospheres, air, humidity, steam, some gases like fuel gases, chlorine, hydrogen sulphide, oxides of nitrogen, ammonia and sulphur (IV) oxide, carbon dioxide, soils, alkalis and acids [8–10]. In the oilfield, acidic fluids, petroleum wastewater, brines, alkalis, microbial rich fluids and some gases constitute the corrosive environments [11]. To monitor corrosion, a selected corrosive environment may be simulated in the laboratory and placed in contact with the metal or alloy for a stipulated contact time. After this time, the metal or alloy substrate (usually in form of a coupon) is cleaned by standard procedures, and the corrosion rate can be evaluated. In this chapter, emphasis will be laid on corrosion in oilfield environments with preference to acidising (HCl) solution.

2. Corrosion in acidising solution

Acid corrosion constitutes the major source of corrosion often encountered in the oilfield. Strong acids can be pumped into wells to increase formation permeability and stimulate production. About 5–28% HCl is commonly used for limestone formations, while hydrogen fluoride (up to 3%) is used for sandstone formations [8]. Also, about 9% formic acid has been used in some deep sour wells where HCl inhibitors lose their effectiveness [1]. These acids in the live and spent forms cause serious corrosion problems.

2.1 Corrosion monitoring and measurement of corrosion rate

Steel is the main material used for construction of pipework in the oilfield. Since the main chemical constituent of steel is iron, the dissolution of iron in acid (HCl) may be illustrated using Eq. (1):

$$Fe(s) + 2HCl(aq) = FeCl2(aq) + H2(g) \quad (1)$$

Therefore, the corrosion of steel may be monitored using the following methods [12]:

- Determining the mass of $Fe_{(s)}$ left (or lost) after dissolution within a given time frame by weight loss (or gravimetric) technique.
- Determining the changes in resistance to charge transfer between the steel surface and the electrolyte which are embedded by electrochemical impedance spectroscopy (EIS).
- Determination of changes in activity or electrochemical potential or resistance using electrochemical techniques.
- Measuring the speed of release of hydrogen gas or the amount released within a time frame by hydrogen evolution or gasometric technique.
- Determining the amount of the Fe(s) leached into the solution at intervals by AAS or EDS and so on.

2.2 Corrosion products analyses

For any of the methods used to monitor the progress of corrosion, the steel specimen has to be immersed in the corroding medium for a given frame of time, then retrieved. Within this time, a measureable extent of corrosion would have occurred and the corrosion products will be present either in the corroding medium (from which the specimen was retrieved) and/or on the retrieved steel surface. At this point, either the solution or the surface or both may be subjected to spectroscopy or other analyses. The proceeding sections will concentrate only on the frequently used spectroscopic methods for corrosion analyses. These are: electrochemical impedance spectroscopy (EIS), ultraviolet/visible (UV-Vis) spectroscopy, FTIR spectroscopy, XRD spectroscopy, EDAX spectroscopy, AAS and XPS.

3. Spectroscopic techniques for corrosion analyses

In this section, our focus will be on the familiar experimental spectroscopic methods used to monitor corrosion and analyse corrosion products in the laboratory. Except where otherwise stated, steel is mainly considered as the substrate/specimen. Most spectroscopic techniques are associated with the interaction of the surface with electromagnetic radiation. Often, direct contact with the specimen may not be necessary. While some of the techniques can be used for *in situ* corrosion monitoring, techniques for detection and analyses of corrosion products are not associated with *in situ* analysis.

3.1 Electrochemical impedance spectroscopy (EIS)

EIS is an experimental method that is based on the measurement of impedance as a function of frequency or angular frequency of a sinusoidal perturbation of small amplitude under steady-state conditions [13]. Since frequency is used as a variable, it is termed as 'spectroscopy'. The measurement is often conducted within a large frequency range that covers several decades, from mHz to hundreds of kHz. Sometimes, the frequency range could cover μHz to MHz.

In immersion tests, the steel coupon is abraded or polished to mirror finishing, cleaned (using standard procedures such as ASTM, NACE, etc.) and soldered to the wire to obtain the working electrode. Often, only one surface (of known area) on the coupon is exposed, while the other surfaces are insulated, often using epoxy adhesives [14]. For some specialised cells, there is no need for soldering to a wire as the cell has a ready compartment (with a hole) for insertion of the coupon. In this case, the coupon 'laps' on a conductor, which connects the coupon with the other components of the cell once the electrolyte is poured into the cell.

On complete connection of the cell to the potentiostat/galvanostat, a green signal shows on the screen to signify that the cell is ready for measurement taking. With EIS, corrosion data may be obtained *in situ*. Many researchers have reported that the cell will be initially allowed to stand for some time so that corrosion can occur and open circuit potential (OCP) may stabilise [15–18]. For instance, the curves in **Figure 1a–b** show variation of OCP with standing time over a period of 30 min. It can be observed that the OCP stabilises for Specimens A and B within 120 s but is unstable for Specimen C even after 1800 s. Once the actual measurement begins, a graphical representation of the measured impedance is obtained at different frequencies. The most frequently used coordinates for presenting impedance data include:

- Plot of frequencies as a set of points in the complex-impedance plane with the real components of impedance (Z') on the x-axis and the imaginary component ($-Z''$) on the y-axis or vice versa. This plot is commonly called Nyquist plot or complex plane diagram, and an example is shown in **Figure 1c**.

- Plots of Z' and $-Z''$ as a function of frequency (usually $\log f$). This presentation is not popular for experimental cases in literature.

- Plots of magnitude of impedance /Z/ or log/Z/ and argZ against $\log f$, often referred to as Bode plot.

The measured data for $Z(w)$ are interpreted by comparison with predictions of a theoretical model or by the use of an equivalent circuit. Use of equivalent circuit is commonly reported [19, 20] and the output parameters are determined depending on the best fitting equivalent circuit. Basically, best fitting of theoretically calculated impedance plots to experimentally obtained curves affords acceptable results if there is sufficiently small deviation (often expressed as χ^2). Charge transfer resistance is obtained at the point of intercept of the curve with the impedance axis. Depending on the equivalent circuit model used, other parameters such as double-layer capacitance, solution resistance, film resistance and (constant phase element) CPE constant may be obtained from the analyses of the EIS spectrum.

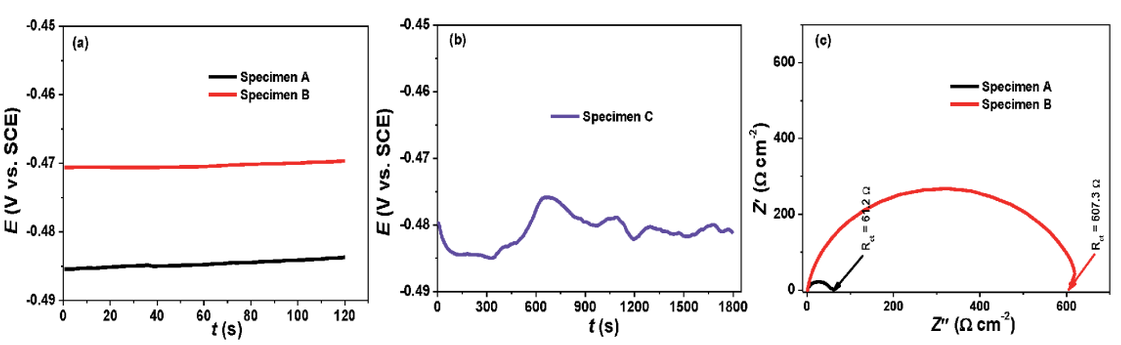

Figure 1.
(a and b) Variation of OCP with time and (c) Nyquist plot.

3.2 UV-Vis spectroscopy

Electromagnetic radiation within the ultraviolet and visible regions produces electronic excitation of molecules in a system. With the use of CIs, electrons move from one energy level to another. Depending on the chemical identity of the CI, excitations could be from the non-bonding (n) orbital (if the CI contains N, O, S and P) or from the pie (π) bonding orbitals (if it contains multiple bonds or aromatic rings) to other allowed orbitals. Such transitions are usually accompanied by the characteristic absorption in the UV-Vis region, resulting in a peak in the spectrum of the CI when scanned by the UV-Vis spectrophotometer. The wavelength(s) of maximum absorption (λ_{max}) may be recorded and used to probe corrosion. Also, formation of a complex between inhibitor species and steel species can result in another absorption and yield of similar or different λ_{max}.

In many corrosion studies, the steel specimen is immersed in the test solution for a period of time for reasonable corrosion to occur, then retrieved [8]. Aliquots of the resulting solution (containing the corrosion products) is diluted and scanned within suitable range of wavelengths [21]. Results produce absorption bands which could be used to predict the associated electronic transition. Often, the results are interpreted based on shifts in the adsorption spectra without and with the inhibitor. Typical UV-Vis spectra obtained by monitoring corrosion of X80 steel in 1 M HCl before and after immersion of steel in the inhibited solution are shown in **Figure 2a**. A shift in the spectral position in the after immersion indicates that there is interaction between the inhibitor and the steel species. Such interactions are often believed to result from the formation of a complex between active sites on the inhibitor molecule and Fe in steel [22, 23]. However, the use of UV-Vis data to predict the corrosion inhibitor-steel surface interaction is limited and considered obsolete because it does not provide explicit mechanistic information like other techniques.

3.3 FTIR spectroscopy

Vibration of functional groups on the interaction with electromagnetic radiation is the bases for application of FTIR in corrosion studies. Since each functional group has a characteristic vibrational frequency, it is easy to deploy this technique to characterise corrosion products, although not *in situ*. The surface of the steel coupon retrieved from the inhibited solution is usually cleaned, and the thin inhibitor film is gently removed. The removed film is therefore tableted with KBr and analysed by

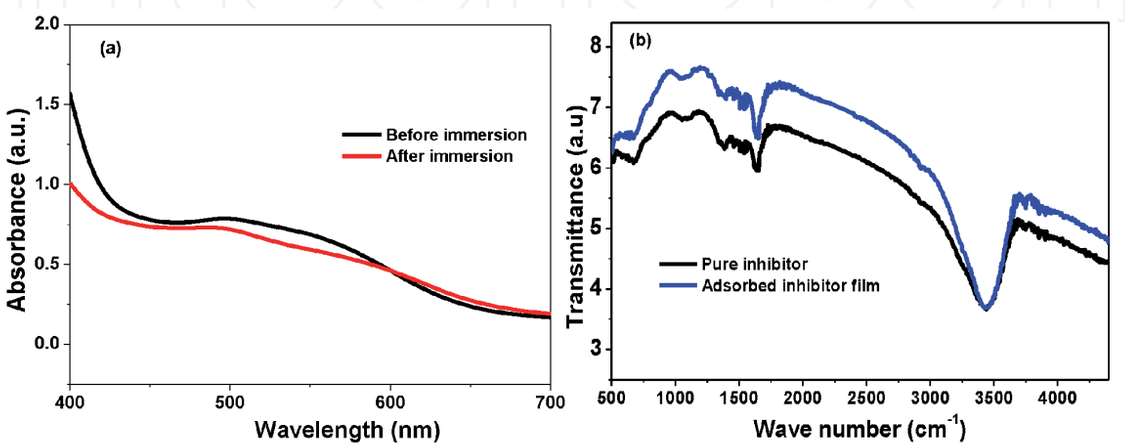

Figure 2.
(a) Typical UV-Vis spectra before and after immersion of X80 steel in 1 M HCl containing a corrosion inhibitor and (b) FTIR spectra of a pure corrosion inhibitor and adsorbed inhibitor film after immersion.

FTIR to obtain a spectrum. This is also repeated using the pure inhibitor material and another spectrum is obtained. Both spectra are often compared and shifts in position of peaks corresponding to vibrational frequencies of associated functionalities are used to predict the mechanism of interaction between the inhibitor and the steel surface [24, 25].

The experimental peaks are often matched with standard IR charts such as that of NIST or Sigma Aldrich. Example of FTIR spectra for a nanoscale bio-based corrosion inhibitor evaluated in 1 M HCl is shown in **Figure 2b**. More information on the prediction of the associated functional groups based on the obtained spectral information is provided in the following application section.

3.4 XRD spectroscopy

XRD provides information on the atomic and molecular structure of crystalline materials. It achieves this by observing the interference patterns resulting from the elastic scattering of X-rays on crystal planes. Recently being deployed for monitoring corrosion and corrosion products analyses, the technique involves scanning the surface of cleaned steel specimens retrieved from inhibited and uninhibited solutions [26]. Since Fe is the main composition of steel, the intensity of Fe obtained in the absence of the inhibitor is expected to be higher. In a recent report, Obot and co-workers observed that the intensity of Fe (100) peak obtained in the presence of inhibitors was lower than without inhibitors. They inferred that the adsorption of the CIs block off the Fe (110) reactive sites, making it less detectable during the XRD characterisation.

3.5 EDAX spectroscopy

Another X-ray technique used to detect corrosion products is the EDS. The surface of a cleaned steel specimen is scanned and the elemental composition on the surface is profiled. Without and with the corrosion inhibitor, the spectral features, percentage composition or abundance of desired elements could be compared. Comparison enables researchers to observe which element has increased in composition or has decreased. The data are therefore correlated to predict the mechanism of interaction between the surface-adsorbed inhibitor and the substrate. For instance, in **Figure 3a**, the EDS spectral features of X80 steel immersed in 1 M HCl is shown, while the one immersed in 1 M HCl containing a particular organic inhibitor (name withheld) is shown in **Figure 3b**. The differences in the spectral profiles have been used to describe the corrosion process in the following application section. Although many recent researches have deployed this method for mechanistic determinations, EDS is considered not sensitive for predicting the interactions of functional groups, except only the elemental composition.

3.6 AAS spectroscopy

When a steel coupon is immersed in a corrosive medium over a duration of time (t), the amount (or concentration) of iron leached into the medium can be determined by AAS. With this, the corrosion rate can be estimated. Suppose this is repeated in the presence of inhibitor compounds, then the corrosion inhibition efficiency can be determined in relation to the uninhibited solution [27]. The surface of the steel is prepared by following a standard method. After immersion, cleaning of the surface is not necessary as the analyses are carried out on the resulting solution containing the corrosion products. AAS presents a kind of *in situ* method for monitoring corrosion whereby aliquots of medium (during the progress of

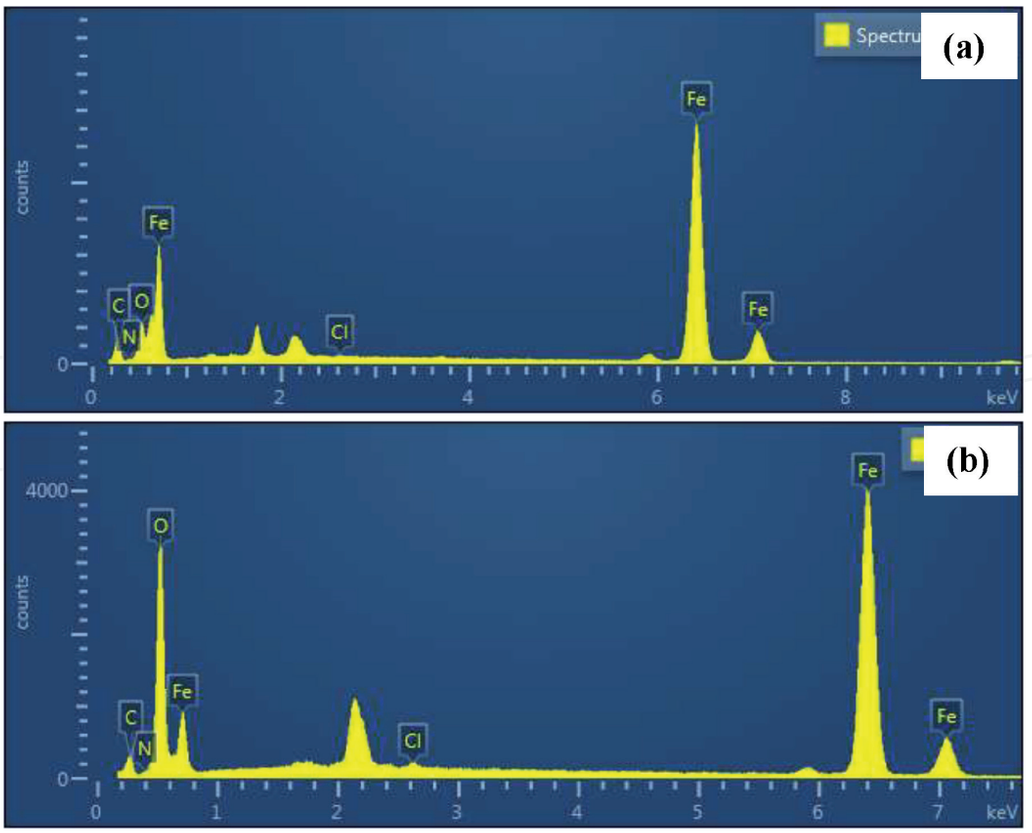

Figure 3.
EDS spectra showing the composition of Fe, C, N, O and Cl on X80 steel surface after immersion in (a) 1 M HCl and (b) 1 M HCl containing an organic corrosion inhibitor.

corrosion) may be taken at regular time interval and analysed. It could be possible to kinetically determine the order and rate constants using this technique. However, it is not often reported because it is regarded as insensitive since only the concentration of iron is used for calculation, whereas other leached metals that constitute the steel are not considered.

3.7 XPS spectroscopy

X-ray photoelectron spectroscopy or electron spectroscopy for chemical analyses (ESCA) is one of the essential tools in corrosion analyses nowadays. With XPS, the composition of a surface and the thickness of a film can be quantitatively estimated [28]. Being non-destructive on the specimen, it can also be used to probe the composition of the steel surface under the surface film. Typical escape depths of XPS experiments are estimated at ca. 3 nm at maximum, with the photoelectrons accelerated at kinetic energies of 100–1500 eV under nitrogen purging. With this, only information on thin surface region may be obtained and in the form of chemical shifts corresponding to different chemical states [29]. Results often generate two types of spectra. The first is called the survey spectrum which shows all the elements present on the specimen surface. The second is often called the deconvoluted spectrum which is used to correlate the type of bond present based on the characteristic binding energy obtained.

4. Application of spectroscopy in corrosion analyses

Spectroscopy plays an important role in corrosion analyses, especially as information on the mechanism of interaction can be derived from a single or

combination of spectroscopic data. For instance, in the study of corrosion inhibition of X80 steel in 1 M HCl using L-theanine as corrosion inhibitor, the mechanism of interaction between the surface and inhibitor was described using FTIR in addition to other quantities such as binding/interaction energy [30]. FTIR results also supported quench molecular dynamics computations and provided insights into the possible adsorption sites at both molecular level and experimentally.

When a protective film is formed by a corrosion inhibitor on the surface of it its substrate, the interaction between the film and the surface is usually facilitated by some active groups in the inhibitor. Usually, the spectrum of the pure inhibitor will be different from that of its surface film. The peaks corresponding to some active groups could disappear, broaden, sharpen or shift to higher or lower wave numbers [31, 32]. The obtained spectra for pure LTN and its surface film are shown in **Figure 4** [30]. The sharp prominent peaks around 1100 cm^{-1} were assigned to C–O or C–N stretch. This peak shifted to 1055 cm^{-1}, indicating that there could have been slight modification due to its involvement in the adsorption process. Similarly, shifts and changes in intensity can be observed with peaks at 1360–1630 and 2930 cm^{-1} which were assigned to C–O stretch, C=O or N–H stretch and O–H or C–H stretch, respectively. It was inferred that such shifts signify that C=O, N–H or O–H sites may have been active in interacting with the steel surface, which could have resulted in the modification of the spectral properties. More conspicuously, the peak at 3460 cm^{-1} assigned to –N–H amine or –O–H (intermolecular bond) was found to become very broad after adsorption, a clear evidence that the sites could have been modified after taking part in the adsorption.

EDS has been widely used to profile steel surface and its corrosion products [33] in addition to FTIR. The spectrum in **Figure 3a** represents the mapped entire surface of a highly corroded surface retrieved from 1 M HCl (**Figure 5a**), whereas the spectrum in **Figure 3b** profiled the highlighted section on the surface retrieved from the inhibited solution (**Figure 5b**). To make proper meaning, the percentage compositions of the respective elements on the surface are displayed in **Table 1**.

From results presented in **Table 1**, the surface is very rich in C and Fe, which are the main elements in steel as well as O perhaps due to the oxidation of surface. This can be confirmed from the higher amounts of Fe, C and O obtained with the uninhibited system. Interaction of surface species with chloride ions in the HCl

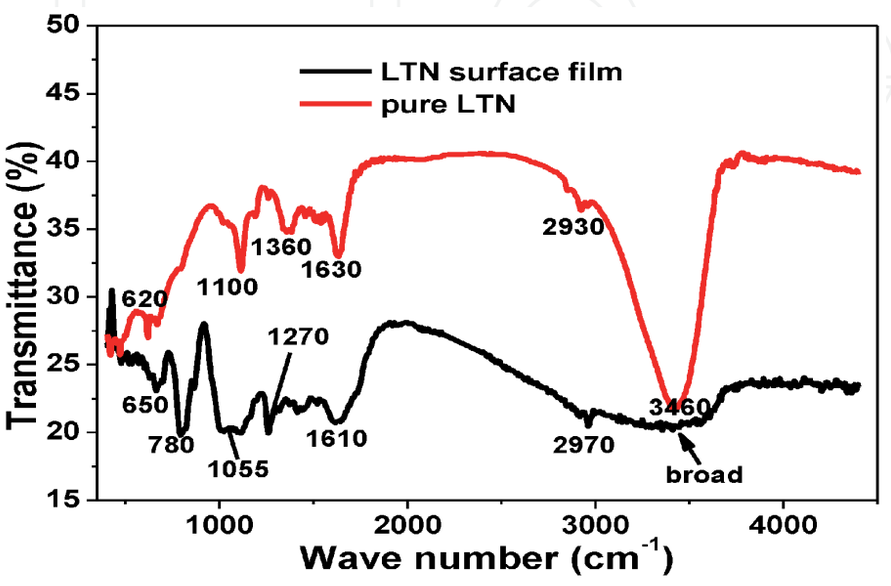

Figure 4.
FTIR spectral profiles of pure LTN, and LTN thin film formed on X80 steel surface [30].

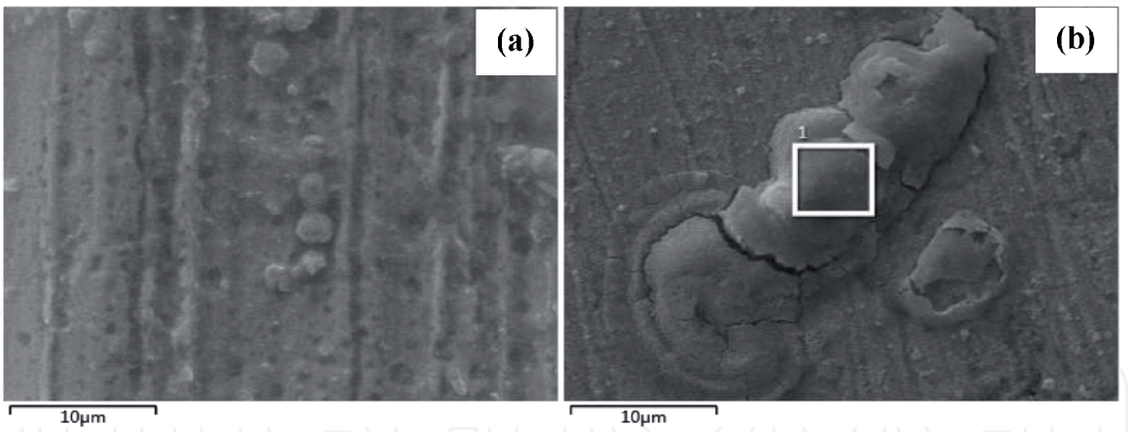

Figure 5.
Surfaces of X80 steel profiled by EDS.

Element	Uninhibited			Inhibited		
	Apparent conc.	Wt.%	Atomic %	Apparent conc.	Wt.%	Atomic %
C	5.08	12.29	26.01	1.29	2.52	8.27
N	0.03	0.12	0.18	0.07	0.26	0.23
Cl	0.46	0.39	0.44	0.23	0.04	0.13
O	12.98	0.17	12.17	33.31	13.02	32.10
Fe	150.98	87.03	61.20	89.94	84.16	59.27

[*] Results of ongoing research (unpublished) by Ekemini Ituen.

Table 1.
Elemental composition of the profiled X80 steel surface retrieved from (a) uninhibited and (b) inhibited 1 M HCl solution[*].

medium also resulted in some amounts of Cl being found on the surface. However, on addition of the organic inhibitor which contains C=C, N and O in its molecular structure, a thin film was formed on the surface which protected it from excessive corrosive attack. This resulted in the reduction in the amounts of C, Cl and Fe 'seen' on the surface due to the 'blanketing' effect of the inhibitor. Instead, the amounts O and N on the surface increased which could have come from the adsorbed inhibitor species. In some reports, the amount of C was found to increase [34, 35], and it was attributed to involvement of C=C sites in the adsorption process.

During the evaluation of a benzimidazole derivative (BPMB) as alternative carbon steel corrosion inhibitor in CO_2-saturated brine solution, the steel surfaces in the uninhibited and inhibited media were analysed by XRD [26]. Obot and co-workers report that the most prominent diffraction peaks were observed at 2θ = 44.9° and 2θ = 65° assigned to Fe (110) and Fe (200) crystallographic phases. Fe (110) plane, being the predominantly oriented and stable plane in steel, showed the highest frequency in the absence of BPMB as shown in **Figure 6a**. On introduction of BPMB to the corroding medium, the intensity of the Fe (110) peak diminished (**Figure 6b**) due to adsorption of BPMB. It was implied that the adsorption of corrosion inhibitors blocked the Fe (110) reactive sites, making it less detectable during XRD characterisation [26].

In **Figure 7a**, a survey spectrum of X80 steel retrieved from 1 M HCl solution and inhibited by the plant extract-mediated silver nanoparticles as analysed by XPS is shown. Analyses of the spectrum with prejudice to Fe shows the presence of C (1s), N (1s), Ag ($^3d_5$), O (1s) at atomic percentages of 68.45, 0.64, 0.14 and 30.76%,

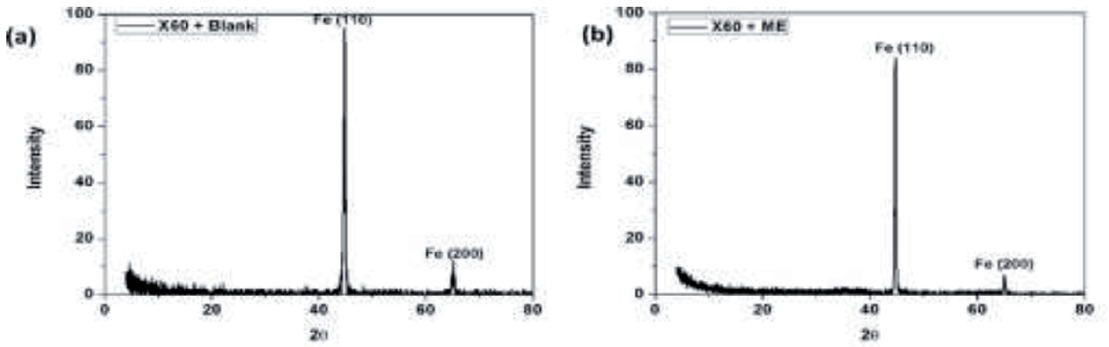

Figure 6.
XRD diffraction pattern of X60 steel retrieved from (a) uninhibited and (b) inhibited acid solution [26].

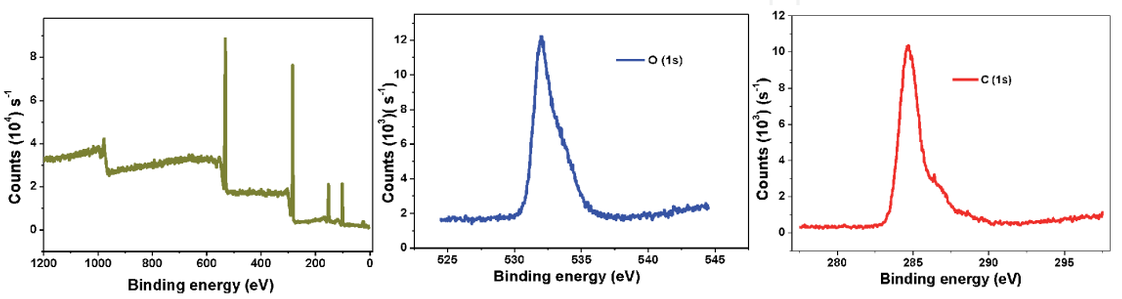

Figure 7.
(a) Survey spectra for the adsorption of onion peel extracts and silver nanoparticles on X80 steel surface in 1 M HCl, and representative spectra for (b) O (1s) and (c) C (1s).

respectively. However, the survey spectrum of the steel surface in the absence of the inhibitor (not shown) yielded no Ag and no N atoms and also lower percentages of C and O on the surface. These demonstrate that the silver nanoparticles were adsorbed on the steel surface, hence the appearance of Ag. The Ag was coordinated to phyto-compounds from the plant extract possibly by means of C=C, C–O, C–N, O–H and C=O sites which enhanced their adsorptive binding on the steel surface. The deconvoluted spectra are illustrated for the C and O associated with the surface as shown in **Figure 7b** and **c**.

Recently, plant-mediated nickel nanoparticles (Ni-EtNPs) have been demonstrated as highly efficient corrosion inhibitor for X80 steel in 1 M HCl [4]. Electrochemical impedance spectroscopy (EIS) was used to probe the corrosion progress and kinetics. It was observed that it took between 300 and 1200 s for OCP to stabilise (**Figure 8a**) depending on the test solution studied. Nyquist plots (**Figure 8b**) yielded depressed semicircles whose diameters increased as concentration of the Ni-EtNPs increased. All the curves showed one relaxation time constant, demonstrating that corrosion mechanism was the same charge transfer-controlled corrosion process in all the test solutions. As Ni-EtNPs increased, the diameter of the depressed semicircle increased corresponding to an increase in charge transfer resistance. The increase in charge transfer resistance was attributed to be caused by adsorption of a thin film of Ni-EtNPs on the steel surface, and hence corrosion inhibition. The possible scenario at the electrode-film-solution interfaces was modelled by using the equivalent circuit, which is composed of the solution resistance (R_s), film resistance (R_f), charge transfer resistance (R_{ct}) and two constant phase elements (CPEs). On analyses using Gamry E-Chem software, the associated parameters (**Table 2**) were obtained.

The obtained values of R_{ct} increased as concentration of Ni-EtNPs increased signifying that the coverage, number of adsorbed species and corrosion inhibition

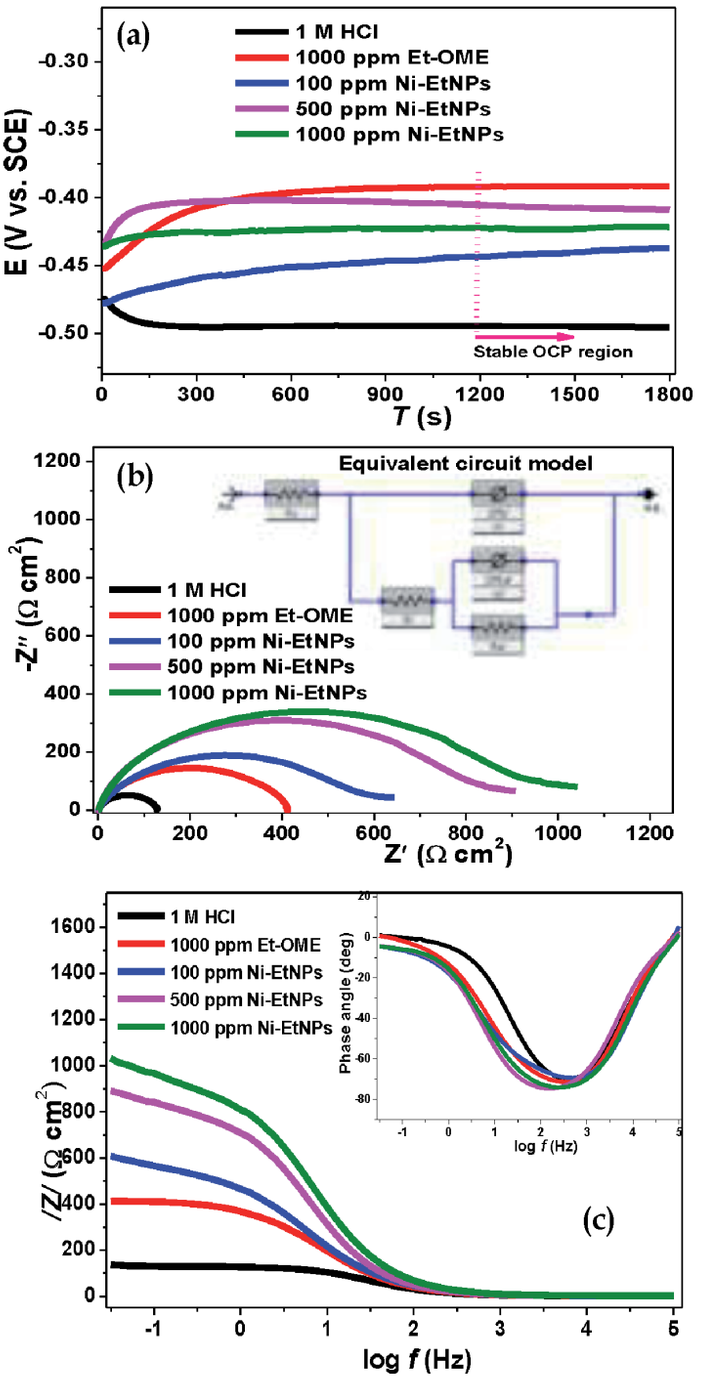

Figure 8.
(a) OCP – Time plot, (b) Nyquist plot with equivalent electrical circuit embedded and (c) bode modulus plot with phase angle plot embedded for the corrosion of X80 steel in 1 M HCl inhibited by various concentrations of Ni-EtNPs at 25°C [4].

increased as concentration increased. The adsorbed Ni-EtNPs species were considered to have formed a surface film with resistance denoted by R_f, which also increased with increase in concentration. By implication, there was increase in the local dielectric or insulation within the region of the surface as a result of adsorption of inhibitor film. As more inhibitor molecules were adsorbed, water molecules were being displaced from the surface leading to decrease in active corrosion sites and reduced corrosion rate. Bode and phase angle plots extracted from obtained impedance data are shown in **Figure 8c**. Values of resistances obtained were consistent with the serial arrangement $R = R_f + R_{ct}$ and were compared to using a crude extract as corrosion inhibitor.

Test solution	R_s (Ωcm^2)	CPE_f				CPE_{dl}		
		n_1	$R_f(\Omega cm^2)$	n_2	$R_{ct}(\Omega cm^2)$	$R(\Omega cm^2)$	χ^2 (x10^{-5})	I_{EIS} (%)
1 M HCl	0.84 ± 0.12	0.84	1.6 ± 0.2	0.70	130.7 ± 1.4	130.2 ± 1.6	0.7	—
1000 ppm Et-OME	0.86 ± 0.10	0.86	11.3 ± 0.2	0.71	389.5 ± 1.6	409.8 ± 2.3	0.8	67.2
100 ppm Ni-EtNPs	0.98 ± 0.11	0.86	17.4 ± 0.2	0.71	686.0 ± 1.4	703.4 ± 2.1	1.5	80.9
500 ppm Ni-EtNPs	0.91 ± 0.15	0.87	24.2 ± 0.3	0.73	954.5 ± 3.2	988.7 ± 2.6	2.9	86.3
1000 ppm Ni-EtNPs	1.08 ± 0.12	0.88	35.1 ± 0.3	0.75	1106.5 ± 3.6	1141.6 ± 4.8	6.2	88.1

Table 2.
EIS parameters for corrosion of X80 steel in 1 M HCl and inhibited by Et-OME and Ni-EtNPs [4].

5. Conclusion

Spectroscopic techniques play key roles in determining monitoring corrosion, analysing corrosion products and predicting mechanism of inhibitor-surface interactions. EIS provides *in situ* information on corrosion rate, corrosion mechanism, charge transfer resistance and double-layer kinetics. UV-Vis provides information on possible formation of a complex between the inhibitor and metal ions from the steel surface signalled by electronic transitions. FTIR and EDS afford information on possible active functionalities on the inhibitor that binds at the surface's active sites, backed up by XPS results. Thus, a combination of the various spectroscopic techniques discussed could be superb for characterising the inhibition of corrosion of steel by a given inhibitor in the acidic oilfield environment.

Author details

Ekemini Ituen[1,2,3], Lin Yuanhua[1,2*], Ambrish Singh[1,2*] and Onyewuchi Akaranta[4]

1 State Key Laboratory of Oil and Gas Reservoir Geology and Exploitation, Southwest Petroleum University, Chengdu, Sichuan, China

2 School of Materials Science and Engineering, Southwest Petroleum University, Chengdu, Sichuan, China

3 Emerging Materials and Energy Research Group, Department of Chemistry, University of Uyo, Uyo, Nigeria

4 African Center of Excellence for Oilfield Chemicals Research, University of Port Harcourt, Port Harcourt, Nigeria

*Address all correspondence to: yhlin28@163.com and vishisigh4uall@gmail.com

IntechOpen

© 2020 The Author(s). Licensee IntechOpen. This chapter is distributed under the terms of the Creative Commons Attribution License (http://creativecommons.org/licenses/by/3.0), which permits unrestricted use, distribution, and reproduction in any medium, provided the original work is properly cited. CC BY

References

[1] Finšgar M, Jackson J. Application of corrosion inhibitors for steels in acidic media for the oil and gas industry: A review. Corrosion Science. 2014;**86**:17-41

[2] Kokalj A, Peljhan S, Finsgar M, Milosev I. What determines the inhibition effectiveness of ATA, BTAH, and BTAOH corrosion inhibitors on copper? Journal of the American Chemical Society. 2010;**132**(46):16657-16668

[3] Sastri VS. Types of corrosion inhibitor for managing corrosion in underground pipelines. In: Underground Pipeline Corrosion. Amsterdam: Woodhead Publishing; 2014. pp. 166-211

[4] Ituen E, Singh A, Yuanhua L. Inhibitive effect of onion mesocarp extract-nickel nanoparticles composite on simultaneous hydrogen production and pipework corrosion in 1 M HCl. International Journal of Hydrogen Energy. 2020;**45**:10814-10825

[5] Ituen E, Mkpenie V, Yuanhua L, Singh A. Inhibition of erosion corrosion of pipework steel in descaling solution using 5-hydroxytryptamine-based additives: Empirical and computational studies. Journal of Molecular Structure. 2020;**1204**:127562

[6] Ituen EB, Akaranta O, Umoren SA. N-acetyl cysteine based corrosion inhibitor formulations for steel protection in 15% HCl solution. Journal of Molecular Liquids. 2017;**246**:112-118

[7] Fabis PM, Brown CW, Rockett T, Heidersbach RH. Infrared and Raman spectroscopic analysis of corrosion products on metals exposed to hydrogen sulfide at elevated temperatures. Journal of Materials for Energy Systems. 1981;**3**(2):66-75

[8] Ahmad Z. Principles of Corrosion Engineering and Corrosion Control. Amsterdam: Elsevier; 2006

[9] Kermani MB, Morshed A. Carbon dioxide corrosion in oil and gas production—A compendium. Corrosion. 2003;**59**(8):659-683

[10] Ren C, Liu D, Bai Z, Li T. Corrosion behavior of oil tube steel in simulant solution with hydrogen sulfide and carbon dioxide. Materials Chemistry and Physics. 2005;**93**(2-3):305-309

[11] Iverson WP. Microbial corrosion of metals. In: Advances in Applied Microbiology. Vol. 32. Cambridge, MA: Academic Press; 1987. pp. 1-36

[12] Choudhry KI, Carvajal-Ortiz RA, Kallikragas DT, Svishchev IM. Hydrogen evolution rate during the corrosion of stainless steel in supercritical water. Corrosion Science. 2014;**83**:226-233

[13] Bard AJ, Inzelt G, Scholz F, editors. Electrochemical Dictionary. New York, NY: Springer Science & Business Media; 2008

[14] Ituen E, Mkpenie V, Ekemini E. Corrosion inhibition of X80 steel in simulated acid wash solution using glutathione and its blends: Experimental and theoretical studies. Colloids and Surfaces A: Physicochemical and Engineering Aspects. 2019;**578**:123597

[15] Ituen E, Ekemini E, Yuanhua L, Singh A. Green synthesis of Citrus reticulata peels extract silver nanoparticles and characterization of structural, biocide and anticorrosion properties. Journal of Molecular Structure. 2020;**1207**:127819

[16] Xu X, Singh A, Sun Z, Ansari KR, Lin Y. Theoretical, thermodynamic and electrochemical analysis of biotin drug

as an impending corrosion inhibitor for mild steel in 15% hydrochloric acid. RSC Advances. 2017;**4**:170933. DOI: 10.1039/C9NJ01691K

[17] Obot IB, Ankah NK, Sorour AA, Gasem ZM, Haruna K. 8-Hydroxyquinoline as an alternative green and sustainable acidizing oilfield corrosion inhibitor. Sustainable Materials and Technologies 2017;14:1-0.

[18] Ituen EB, James AO, Akaranta O. Fluvoxamine-based corrosion inhibitors for J55 steel in aggressive oil and gas well treatment fluids. Egyptian Journal of Petroleum. 2017;**26**(3):745-756

[19] Yuan X-Z, Song C, Wang H, Zhang J. Electrochemical Impedance Spectroscopy in PEM Fuel Cells. Springer London; 2010. DOI: 10.1007/978-1-84882-846-9

[20] Jia WA, Mengyang JI, Zhaohui YA, Bing HA. On completeness of EIS equivalent circuit analysis for electrochemical corrosion process. Journal of the Chinese Society of Corrosion and Protection. 2018;**37**(6):479-486

[21] Li Y, He JB, Zhang M, He XL. Corrosion inhibition effect of sodium phytate on brass in NaOH media. Potential-resolved formation of soluble corrosion products. Corrosion Science. 2013;**74**:116-122

[22] Vinutha MR, Venkatesha TV. Review on mechanistic action of inhibitors on steel corrosion in acidic media. Portugaliae Electrochimica Acta. 2016;**34**(3):157-184

[23] Shainy KM, Ammal PR, Unni KN, Benjamin S, Joseph A. Surface interaction and corrosion inhibition of mild steel in hydrochloric acid using pyoverdine, an eco-friendly bio-molecule. Journal of Bio- and Tribo-Corrosion. 2016;**2**(3):20

[24] Alaneme KK, Olusegun SJ, Adelowo OT. Corrosion inhibition and adsorption mechanism studies of Hunteria umbellata seed husk extracts on mild steel immersed in acidic solutions. Alexandria Engineering Journal. 2016;**55**(1):673-681

[25] Chitra S, Anand B. Surface morphological and FTIR spectroscopic information on the corrosion inhibition of drugs on mild steel in chloride environment. Journal of Chemical and Pharmaceutical Sciences. 2017;**10**:453-456

[26] Obot IB, Onyeachu IB, Umoren SA. Alternative corrosion inhibitor formulation for carbon steel in CO2-saturated brine solution under high turbulent flow condition for use in oil and gas transportation pipelines. Corrosion Science. 2019;**159**:108140

[27] Ituen E, Akaranta O, James A. Green anticorrosive oilfield chemicals from 5-hydroxytryptophan and synergistic additives for X80 steel surface protection in acidic well treatment fluids. Journal of Molecular Liquids. 2016;**224**:408-419

[28] Asami K, Hashimoto K. X-ray photoelectron spectroscopy for corrosion studies. Langmuir. 1987;**3**(6):897-904

[29] Walczak MS, Morales-Gil P, Belashehr T, Kousar K, Lozada PA, Lindsay R. Determining the chemical composition of corrosion inhibitor/metal interfaces with XPS: Minimizing post immersion oxidation. Journal of Visualized Experiments. 2017;**121**:e55163

[30] Ituen E, Mkpenie V, Dan E. Surface protection of steel in oil well acidizing fluids using L-theanine-based corrosion inhibitor formulations: Experimental and theoretical evaluation. Surface and Interface Analysis. 2019;**16**:29-42

[31] Salarvand Z, Amirnasr M, Talebian M, Raeissi K, Meghdadi S. Enhanced corrosion resistance of mild steel in 1 M HCl solution by trace amount of 2-phenylbenzothiazole derivatives: Experimental, quantum chemical calculations and molecular dynamics (MD) simulation studies. Corrosion Science. 2017;**114**:133-145

[32] Ameh PO. A comparative study of the inhibitory effect of gum exudates from *Khaya senegalensis* and *Albizia ferruginea* on the corrosion of mild steel in hydrochloric acid medium. International Journal of Metals [Internet]. Hindawi Limited. 2015;**2015**:1-13. DOI: 10.1155/2015/824873

[33] Ituen E, Akaranta O, James A. Electrochemical and anticorrosion properties of 5-hydroxytryptophan on mild steel in a simulated well-acidizing fluid. Journal of Taibah University for Science. 2017;**11**(5):788-800

[34] Ituen E, Ekemini E, Yuanhua L, Li R, Singh A. Mitigation of microbial biodeterioration and acid corrosion of pipework steel using Citrus reticulata peels extract mediated copper nanoparticles composite. International Biodeterioration and Biodegradation. 2020;**149**:104935

[35] Ituen E, Singh A, Li R, Yuanhua L, Guo C. Nanostructure, surface and anticorrosion properties of phyto-fabricated copper nanocomposite in simulated oilfield descaling fluid. Surface and Interface Analysis. 2020;**3**:100514